Impact of doped barriers on the recombination coefficients of c-plane InGaN/GaN single quantum well light-emitting diodes

Y C Chow, C. Lynsky, S. Nakamura, S P Denbaars, C. Weisbuch, J S Speck

Applied Physics Letters

RESEARCH ARTICLE | NOVEMBER 01 2022

Impact of doped barriers on the recombination coefficients of *c*-plane InGaN/GaN single quantum well light-emitting diodes

Y. C. Chow ; C. Lynsky ; S. Nakamura ; S. P. DenBaars ; C. Weisbuch; J. S. Speck

Appl. Phys. Lett. 121, 181102 (2022)
https://doi.org/10.1063/5.0117318

Applied Physics Letters ARTICLE scitation.org/journal/apl

Impact of doped barriers on the recombination coefficients of c-plane InGaN/GaN single quantum well light-emitting diodes

Cite as: Appl. Phys. Lett. **121**, 181102 (2022); doi: 10.1063/5.0117318
Submitted: 31 July 2022 · Accepted: 5 October 2022 ·
Published Online: 1 November 2022

Y. C. Chow,[1,a)] C. Lynsky,[1] S. Nakamura,[1,2] S. P. DenBaars,[1,2] C. Weisbuch,[1,3] and J. S. Speck[1]

AFFILIATIONS

[1]Materials Department, University of California, Santa Barbara, California 93106, USA
[2]Department of Electrical and Computer Engineering, University of California, Santa Barbara, California 93106, USA
[3]Laboratoire de Physique de la Matière Condensée, CNRS, Ecole Polytechnique, IP Paris, 91128 Palaiseau, France

[a)]Author to whom correspondence should be addressed: yichao@ucsb.edu

ABSTRACT

Differential carrier lifetime measurements were performed on *c*-plane InGaN/GaN single quantum well (QW) light-emitting diodes (LEDs) of different QW indium compositions as well as with and without doped barriers. Mg-doped *p*-type and Si-doped *n*-type barriers close to the QW were used to reduce the net internal electric field in the QW, thereby improving the electron–hole wavefunction overlap on the LEDs. LEDs with doped barriers show short lifetimes and low carrier densities in the active region compared to the reference LEDs. The recombination coefficients in the ABC model were estimated based on the carrier lifetime and quantum efficiency measurements. The improvement in the radiative coefficients in the LEDs with doped barriers coupled with the blueshift of the emission wavelengths indeed indicates an enhancement in wavefunction overlap and a reduction of quantum confined Stark effect as a result of the reduced internal electric field. However, doped barriers also introduce non-radiative recombination centers and thereby increase the Shockley–Read–Hall (SRH) coefficient, although the increment is less for LEDs with high indium composition QWs. As a result, at high indium composition (22%), LEDs with doped barriers outperform the reference LEDs even though the trend is reversed for LEDs with lower indium composition (13.5%). Despite the trade-off of higher SRH coefficients, doped barriers are shown to be effective in reducing the internal electric field and increasing the recombination coefficients.

Polarization-induced electric fields in *c*-plane InGaN/GaN quantum wells (QWs) are deleterious to the light-emitting diodes (LEDs), especially for emitters with high indium composition. For the most common Ga-polar *c*-plane LEDs with p-side-up geometry, the polarization-induced electric field in the QW is much larger than the opposite *p*–*n* junction electric field, resulting in a large net internal electric field in the QWs. This causes reduced overlap of the electron and hole wavefunctions,[1–4] decreasing the recombination coefficients that relate to the internal quantum efficiency (IQE) of the LEDs through a simple ABC model: $IQE = Bn^2/(An + Bn^2 + Cn^3)$, where n is the active region carrier density and A, B, and C are the coefficients for Shockley–Read–Hall (SRH), radiative, and Auger recombination, respectively. While some compensation occurs between the decreases in radiative and non-radiative coefficients in determining the maximum IQE,[5] the decrease in all recombination coefficients leads to higher n at a given current density and, thus, the onset of efficiency droop at lower current densities.

Theoretical and experimental efforts have shown that it is possible to reduce the internal electric fields in the *c*-plane InGaN/GaN QWs through the use of doped barriers.[6–10] Placing heavily doped *p*- and *n*-type GaN barriers close to the QW leads to an increase in the *p*–*n* junction electric field, which counteracts the opposite polarization-induced electric field in the QW, resulting in a smaller net internal electric field. The technique has been employed in thick *c*-plane single QW LEDs, where thick QW (9 nm) LEDs with low efficiency droop were demonstrated.[10] In this paper, doped barriers were used in thin QW (3 nm) LEDs with different indium compositions. Small-signal measurements were performed on the LEDs under electrical injection to extract the differential carrier lifetimes. Both electrical and optical responses were measured simultaneously to account for the carrier transport effects in the LEDs.[11] Coupled with the quantum efficiency measurements, the recombination coefficients of the LEDs were calculated to understand the effects of doped barriers on the LEDs.

The samples were grown by metalorganic chemical vapor deposition (MOCVD) on *c*-plane patterned sapphire substrates (PSSs). The epitaxial structure was similar to that of the LEDs reported previously,[10] which began with a 2 μm thick unintentionally doped (UID) GaN template layer, a 2 μm n-GaN layer, a 20-period n-$In_{0.04}Ga_{0.96}N$/GaN 2.2 nm/4.5 nm superlattice, and a 30 nm n-GaN layer. The undoped InGaN single QW was capped by a 2 nm undoped GaN layer and sandwiched either between a 12 nm n-type GaN barrier ([Si] = 1.5×10^{19} cm^{-3}) and a 10 nm p-type GaN barrier ([Mg] = 1.7×10^{19} cm^{-3}), or UID GaN barriers of the same thicknesses. The structure was then ended with a 26 nm p-$Al_{0.10}Ga_{0.90}N$ electron blocking layer (EBL), a 100 nm p-GaN, and a 10 nm p$^+$-GaN contact layer. InGaN QWs with three different compositions (13.5%, 16%, and 22%) were grown, and the corresponding LEDs were denoted as LED-V, LED-B, and LED-G, according to their violet, blue, and green light emission, respectively. For every indium composition, two LEDs were grown: one with and the other without doped barriers. These two LEDs have a suffix of "D" (doped) and "R" (reference), respectively [e.g., LED-BD and LED-BR correspond to the blue LEDs ([In] = 16%) with and without doped barriers, respectively].

The samples were processed into devices of two sizes. The larger devices (0.1 mm^2 active area) were mounted on silver headers, wire bonded, and encapsulated in silicone to improve the light extraction efficiency (LEE). The packaged devices were tested in a calibrated integrating sphere from 1 to 400 A/cm^2 to determine the external quantum efficiency (EQE). Pulsed conditions (3%–5% duty cycle with 10 μs pulse widths) were used for testing above 50 A/cm^2 to minimize heating. The IQE of the LEDs was estimated by assuming a light extraction efficiency (LEE) of 80% based on ray tracing simulations[12] (i.e., IQE = EQE/LEE). Smaller devices with circular mesas (40 μm diameter) were used for differential carrier lifetime measurements. During the measurement, a small-signal voltage (100 mV) from a network analyzer (PNA-X N5247A) was added to a DC bias using a bias tee and then applied to the LEDs using a RF probe (ACP40-GS-50). The small-signal frequency was swept from 10 to 500 MHz. The modulated output light was then collected using an optical fiber and fed into a high-speed silicon photodetector (UPD-200-UP). Following this, the signal was amplified by a low noise amplifier and sent back to the network analyzer. To account for the frequency response of the photodetector and amplifier, the response was measured separately by a high-speed laser and subtracted from the response of the LEDs. Differential carrier lifetimes of the LEDs were then obtained by fitting the input impedance [Fig. 1(a)] and modulation response [Fig. 1(b)] of the LEDs using a rate equation-based recombination model described in Ref. 11.

We first compare the measured EQE of the six LEDs, as shown in Fig. 2(a). At the low indium content of 13.5%, the LED with doped barriers (LED-VD) has lower efficiency than the reference LED (LED-VR). This is because the doped barriers also introduce defect-related non-radiative recombination centers (NRCs), which enhance the non-radiative recombination coefficient.[7,10,13,14] However, the increasing indium content reduces the EQE difference between LEDs with and without doped barriers. Although LED-BD has a lower peak EQE (36%) than the reference LED-BR (which has a peak EQE of 45%), it has higher EQE at high current densities (>100 A/cm^2). For the highest indium content in this study (22%), with doped barriers, LED-GD has higher efficiency than its counterpart (LED-GR) regardless of

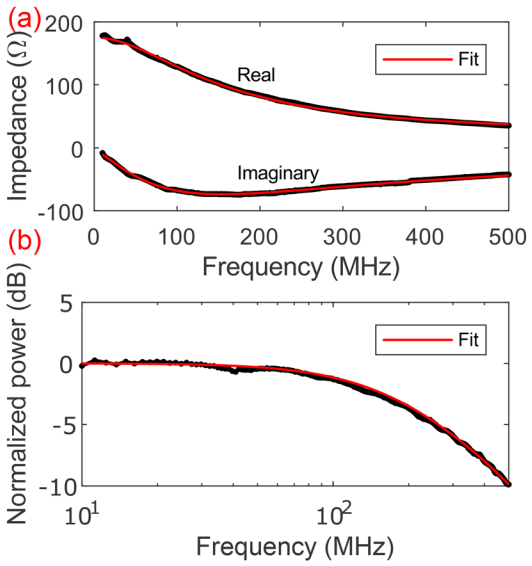

FIG. 1. (a) The real and imaginary parts of the input impedance and (b) the modulation response of LED-BD at 200 A/cm^2. Black dots and lines: experimental data; red lines: model.

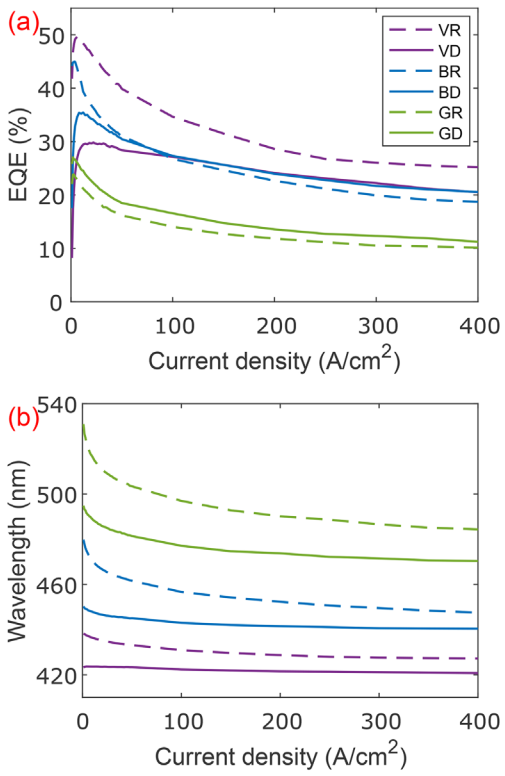

FIG. 2. (a) External quantum efficiency and (b) EL peak wavelength vs current density of the LEDs with (VD, BD, and GD) and without doped barriers (VR, BR, and GR).

current densities. It seems that the higher NRCs, due to the doped barriers, impact the LEDs with high-composition QWs less than that with low-composition QWs.

The dependence of the electroluminescence (EL) peak wavelengths on the current density is shown in Fig. 2(b). As expected, LEDs with doped barriers have shorter emission wavelengths due to the reduced quantum confined Stark effect (QCSE) from reduced internal electric fields. On top of that, they also exhibit smaller variation in wavelengths with respect to the current density due to the reduced internal electric field to be screened by injected carriers, consistent with previous results.[7,10]

Figure 3(a) shows the dependence of the differential carrier lifetime of the LEDs on the current density. For the same indium content, the lifetimes of LEDs with doped barriers are approximately 50% shorter than that of the reference LEDs. It is possible that shorter lifetimes can solely be due to the higher SRH coefficient as a result of defects introduced by the doped barriers. However, as we shall see in the subsequent analysis, the shorter lifetimes are the combination of both higher radiative and non-radiative recombination coefficients in the LEDs with doped barriers.

With differential carrier lifetime (τ), the carrier density (n) can then be determined using the following integral:[5]

$$n = \int_0^G \tau \, dG, \tag{1}$$

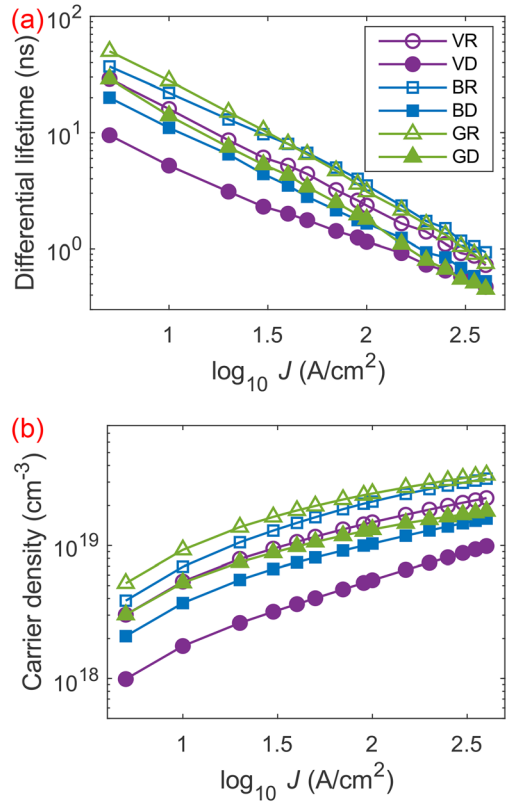

FIG. 3. (a) The extracted differential carrier lifetimes and (b) carrier density from Eq. (1) vs current density of the LEDs.

where $G = (J/qh)$, J, q, and h are the total generation rate, current density, electron charge, and active region thickness, respectively. Although the evaluation of n requires τ at zero current density (τ_0), in actuality, τ can only be measured down to a minimum current density. Thus, the usual procedure is to extrapolate τ and assume τ to be constant at low current density where SRH-dominated regime is reached. Unfortunately, τ did not plateau even at the smallest current density in the measurement. Instead, n was calculated by choosing τ_0 to be τ measured at the lowest current density (5 A/cm^2 in this study). Since the actual τ_0 should be higher than the value used in the calculation, the calculated n can be seen as the lower bound of the actual values. Figure 3(b) shows the calculated n of the LEDs. As expected, LEDs with doped barriers also have a lower n at a given current density due to the shorter τ.

At steady state, G is also the total recombination rate. After separating G into a radiative rate ($G_R = G \times \mathrm{IQE}$) and a non-radiative rate [$G_{NR} = G \times (1 - \mathrm{IQE})$], the recombination coefficients in the simple ABC model, namely, the SRH (A), radiative (B), and Auger (C) coefficients, can then be estimated following the work of David *et al.*[5,15] Three recombination quantities were calculated: G_{NR}/n, $B = G_R/n^2$, and $C = (G_{NR} - An)/n^3$, where A is the value of G_{NR}/n at low current density where the Auger recombination is negligible because of its n^3 dependence. On top of the standard non-radiative SRH recombination and Auger recombination, there could be other possible non-radiative recombination mechanisms. Trap-assisted Auger recombination (TAAR) has been observed by electron emission spectroscopy[16] as well as forward-bias photocurrent measurement[17] and was invoked as a source of green gap by David *et al.*[15] However, we do not have an independent way to introduce defects in otherwise identical structures in this study as the introduction of doped barriers not only increases the NRCs but also enhances the wavefunction overlap. Since it is difficult to decouple the TAAR effect from the other recombination processes in the ABC model, we do not consider TAAR in this study.

The three calculated quantities are shown in Fig. 4 as functions of n. The quantity G_{NR}/n has been commonly reported to converge to a constant value at low current densities, which should be equal to their SRH coefficient A.[18,19] In Fig. 4(a), G_{NR}/n decreases with decreasing n and shows signs of convergence. The values at the lowest n are assumed to be the SRH coefficients. (While more data points at lower n should improve the accuracy of the SRH coefficients, it should not change the conclusion of the subsequent analysis.) In Figs. 4(b) and 4(c), the radiative and Auger coefficients B and C are carrier dependent as reported in similar experiments.[18,20,21] An enhancement of B at low n and high n, which can be explained by Coulomb interaction and free carrier screening, respectively, is observed for all LEDs.[20] A reduction in B at high n due to phase-space filling has also been reported in literature,[19] but it is not noticeable here except in LED-VD where a slight reduction in B can be observed at high n. In most LEDs, the enhancement of B as a result of free carrier screening at high n possibly counteracts the phase-space filling effect.[18] There is a significant correlation between the B and C as functions of carrier density, the In content, and the presence or absence of doped barriers since the wavefunction overlap affects both recombination processes.[21,22] The values of B and C are averaged over the measured range and are shown in the inset of Fig. 4(c). We found that the increase in B is accompanied by an increment of C similar to what was reported in Ref. 21.

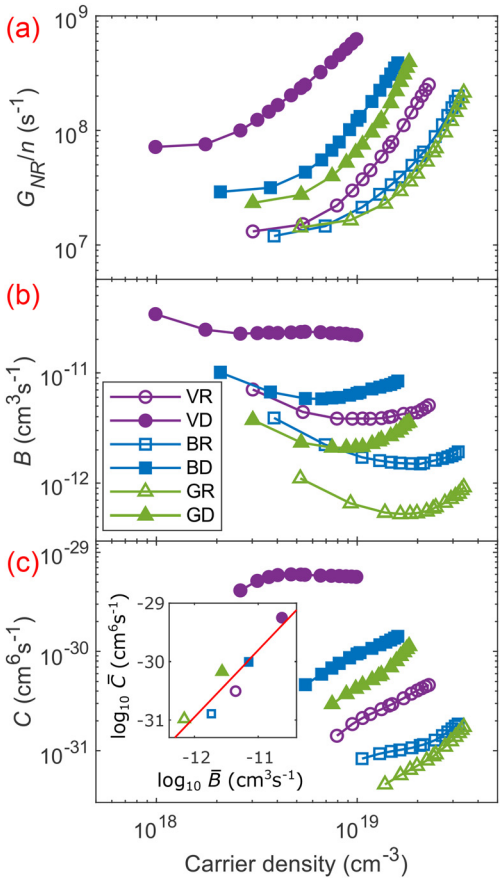

FIG. 4. (a) G_{NR}/n (the value at low J yields SRH coefficient A), (b) the radiative coefficient B, and (c) the Auger coefficient C as a function of carrier density. Inset: the correlation between the average B and C (on a log–log scale).

In Fig. 5, A and the average values of B are also plotted as a function of indium composition. (Note that B is a carrier-dependent quantity. Here, the average values of B are used for ease of comparison between different LEDs in this study.) As seen in Fig. 5(b), B decreases with increasing indium composition. This is expected as the higher polarization-induced electric field in higher indium composition QW results in an even smaller wavefunction overlap, which, in turn, leads to a reduced radiative transition rate. Most importantly, the presence of doped barriers in the LEDs leads to higher radiative coefficients, where an enhancement of four to five times was observed. The higher radiative coefficients are strong indicators that doped barriers lead to reduction in internal electric fields in the QWs, which is their desired effect.

As mentioned above, doped barriers also introduce NRCs, which lead to a higher detrimental SRH coefficient. Higher A, indeed, is observed for all LEDs with doped barriers. The work to identify the defects responsible for the more numerous NRCs is in progress with Mg-related defects as one of the candidates. It is also known that SRH recombination shows strong dependence on wavefunction overlap.[22,23] The improved wavefunction overlap in LEDs with doped barriers further exacerbated the non-radiative SRH recombination.

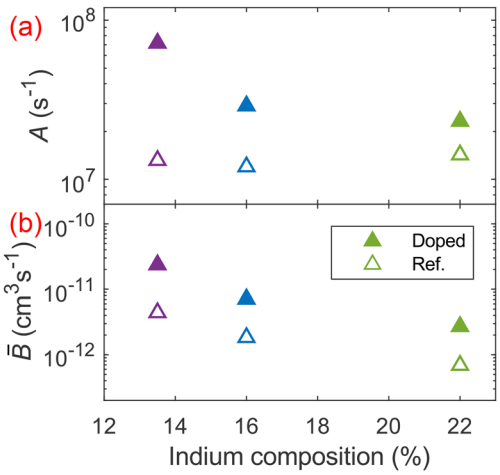

FIG. 5. (a) SRH coefficient A and (b) average radiative coefficient B as a function of indium composition.

However, the increase in A is observed to be smaller with increasing indium composition (5.5 times and 1.6 times higher for violet and green LEDs, respectively). This is not surprising as it was reported that in high-composition QWs, the overlap dependence of SRH coefficients is less pronounced possibly due to a change in the physics governing SRH recombination.[15] Additionally, even without the doped barriers, since NRCs increase with increasing indium composition,[24] the additional NRCs from the doped barriers contribute to a smaller fraction of the total NRCs in the QW with higher indium composition. As such, the penalty associated with the doped barriers is less severe for high-composition QWs. This explains the observed EQE trend, where the LED with doped barriers outperforms the reference LED at high indium composition.

In general, the beneficial enhancement in B is accompanied by the unwanted increase in the non-radiative coefficients A and C partly due to the similar overlap dependence of these non-radiative recombination processes. Nonetheless, the larger recombination coefficients result in a decrease in n at a given injected current density, as shown in Fig. 3(b). The reduced n should delay the efficiency droop onset to higher current densities[5,7] although only slight improvement in efficiency was observed for LED-BD and LED-GD at high current densities.

The shorter carrier lifetimes or faster recombination dynamics in LEDs with doped barriers also enhances their modulation bandwidths, making them suitable for high-speed applications in visible light communication (VLC). 3-dB bandwidths of 284, 265, and 347 MHz were demonstrated by LED-VD, LED-BD, and LED-GD, respectively, at 400 A/cm^2, whereas the bandwidths of the reference LEDs are around 165 to 206 MHz at the same current density (see the supplementary material for more information).

A major drawback in employing doped barriers in LEDs is the blueshifted emission wavelengths. The reduction in the internal electric field leads to a flatter energy band in the QW. This decreases the field-induced redshift, resulting in emitted photons with energies closer to the flatband values. Therefore, a shorter emission wavelength is an unavoidable consequence of reducing the internal electric field in the QW, making this technique to be less optimal for achieving long

wavelength emitters in the visible range. Despite that, this approach is not only limited to InGaN/GaN QW. It can also be applied to AlGaN-based UV emitters, where a shorter emission wavelength is desirable and the large internal electric field in the QW remains a problem.[25]

In conclusion, through the use of doped barriers, we studied the impact of reduced internal electric fields on the recombination coefficients in the QW. Higher recombination coefficients *A*, *B*, and *C* were observed in the LEDs with doped barriers due to their dependence on wavefunction overlap. Doped barriers also introduce additional NRCs which further enhance the *A* coefficients, although the effect is less for high-composition QWs, resulting in the efficiency of the LEDs with doped barriers to exceed that of the reference LEDs. Despite the higher SRH coefficients, doped barriers present another approach to manipulate the internal electric fields in *c*-plane InGaN/GaN QWs.

See the supplementary material for the measured frequency response and 3-dB bandwidths of the LEDs.

This work was supported by the Solid State Lighting and Energy Electronics Center (SSLEEC); the Simons Foundation [Grant Nos. 601952 (J.S.S.) and 601954 (C.W.)]; the National Science Foundation (NSF) RAISE program (Grant No. DMS-1839077); the U.S. Department of Energy under Award Nos. DE-EE0008204 and DE-EE0009691, Sandia National Laboratories (Award No. 2150283); and UCSB-Collaborative Research in Engineering, Science and Technology (CREST). A portion of this work was performed in the UCSB Nanofabrication Facility, an open access laboratory.

AUTHOR DECLARATIONS

Conflict of Interest

The authors have no conflicts to disclose.

Author Contributions

Y. C. Chow: Conceptualization (equal); Formal analysis (lead); Investigation (lead); Methodology (lead); Writing – original draft (lead). **C. Lynsky:** Investigation (supporting); Methodology (supporting). **S. Nakamura:** Funding acquisition (equal); Resources (equal). **S. P. DenBaars:** Funding acquisition (equal); Resources (equal). **C. Weisbuch:** Conceptualization (equal); Funding acquisition (equal); Methodology (equal); Resources (equal); Writing – review & editing (equal). **J. S. Speck:** Conceptualization (equal); Funding acquisition (equal); Methodology (equal); Project administration (lead); Resources (equal); Writing – review & editing (equal).

DATA AVAILABILITY

The data that support the findings of this study are available from the corresponding author upon reasonable request.

REFERENCES

[1]S. F. Chichibu, A. C. Abare, M. P. Mack, M. S. Minsky, T. Deguchi, D. Cohen, P. Kozodoy, S. B. Fleischer, S. Keller, J. S. Speck, J. E. Bowers, E. Hu, U. K. Mishra, L. A. Coldren, S. P. DenBaars, K. Wada, T. Sota, and S. Nakamura, Mater. Sci. Eng.: B **59**, 298 (1999).
[2]J. Seo Im, H. Kollmer, J. Off, A. Sohmer, F. Scholz, and A. Hangleiter, Phys. Rev. B **57**, R9435 (1998).
[3]A. David and M. J. Grundmann, Appl. Phys. Lett. **97**, 033501 (2010).
[4]M. Buongiorno Nardelli, K. Rapcewicz, and J. Bernholc, Appl. Phys. Lett. **71**, 3135 (1997).
[5]A. David, N. G. Young, C. Lund, and M. D. Craven, ECS J. Solid State Sci. Technol. **9**, 016021 (2020).
[6]V. Fiorentini, F. Bernardini, F. Della Sala, A. D. Carlo, and P. Lugli, Phys. Rev. B **60**, 8849 (1999).
[7]N. G. Young, R. M. Farrell, S. Oh, M. Cantore, F. Wu, S. Nakamura, S. P. DenBaars, C. Weisbuch, and J. S. Speck, Appl. Phys. Lett. **108**, 061105 (2016).
[8]T. Deguchi, A. Shikanai, K. Torii, T. Sota, S. Chichibu, and S. Nakamura, Appl. Phys. Lett. **72**, 3329 (1998).
[9]G. Franssen, T. Suski, P. Perlin, R. Bohdan, A. Bercha, W. Trzeciakowski, I. Makarowa, P. Prystawko, M. Leszczyński, I. Grzegory, S. Porowski, and S. Kokenyesi, Appl. Phys. Lett. **87**, 041109 (2005).
[10]Y. C. Chow, C. Lynsky, F. Wu, S. Nakamura, S. P. DenBaars, C. Weisbuch, and J. S. Speck, Appl. Phys. Lett. **119**, 221102 (2021).
[11]A. Rashidi, M. Nami, M. Monavarian, A. Aragon, K. DaVico, F. Ayoub, S. Mishkat-Ul-Masabih, A. Rishinaramangalam, and D. Feezell, J. Appl. Phys. **122**, 35706 (2017).
[12]C. L. Keraly, L. Kuritzky, M. Cochet, and C. Weisbuch, in *III-Nitride Based Light Emitting Diodes and Applications*, edited by T.-Y. Seong, J. Han, H. Amano, and H. Morkoç (Springer Singapore, Singapore, 2017), pp. 301–340.
[13]U. Kaufmann, M. Kunzer, H. Obloh, M. Maier, C. Manz, A. Ramakrishnan, and B. Santic, Phys. Rev. B **59**, 5561 (1999).
[14]A. Nirschl, M. Binder, M. Schmid, I. Pietzonka, H.-J. Lugauer, R. Zeisel, M. Sabathil, D. Bougeard, and B. Galler, Opt. Express **24**, 2971 (2016).
[15]A. David, N. G. Young, C. A. Hurni, and M. D. Craven, Phys. Rev. Appl. **11**, 31001 (2019).
[16]D. J. Myers, K. Gelžinytė, A. I. Alhassan, L. Martinelli, J. Peretti, S. Nakamura, C. Weisbuch, and J. S. Speck, Phys. Rev. B **100**, 125303 (2019).
[17]A. C. Espenlaub, D. J. Myers, E. C. Young, S. Marcinkevičius, C. Weisbuch, and J. S. Speck, J. Appl. Phys. **126**, 184502 (2019).
[18]A. David, N. G. Young, C. A. Hurni, and M. D. Craven, Appl. Phys. Lett. **110**, 253504 (2017).
[19]A. David and M. J. Grundmann, Appl. Phys. Lett. **96**, 103504 (2010).
[20]A. David, N. G. Young, and M. D. Craven, Phys. Rev. Appl. **12**, 44059 (2019).
[21]A. David, N. G. Young, C. Lund, and M. D. Craven, Appl. Phys. Lett. **115**, 193502 (2019).
[22]E. Kioupakis, Q. Yan, and C. G. de Walle, Appl. Phys. Lett. **101**, 231107 (2012).
[23]A. David, C. A. Hurni, N. G. Young, and M. D. Craven, Appl. Phys. Lett. **111**, 233501 (2017).
[24]A. M. Armstrong, M. H. Crawford, and D. D. Koleske, Appl. Phys. Express **7**, 032101 (2014).
[25]M. H. Crawford, in *III-Nitride Semiconductor Optoelectronics*, edited by Z. Mi and C. Jagadish (Elsevier, 2017), pp. 3–44.